Electrically induced and thermally erased properties of side-chain liquid crystalline polymer/liquid crystal/chiral dopant composites

Hua Huang[a]; Jun Geng[a]; Simin He[a]; Bofu Li[a]; Canbin Ouyang[a]; Yuhai Yin[a]; Hui Cao[a]; Liping Wang[a]; Mingtan Hai[a]; Ge Wang[a]; Huai Yang[a]

[a] Department of Materials Physics and Chemistry, School of Materials Science and Engineering, University of Science and Technology Beijing, Beijing 100083, PR China

PLEASE SCROLL DOWN FOR ARTICLE

Electrically induced and thermally erased properties of side-chain liquid crystalline polymer/liquid crystal/chiral dopant composites

HUA HUANG, JUN GENG, SIMIN HE, BOFU LI, CANBIN OUYANG, YUHAI YIN, HUI CAO, LIPING WANG, MINGTAN HAI, GE WANG and HUAI YANG*

Department of Materials Physics and Chemistry, School of Materials Science and Engineering, University of Science and Technology Beijing, Beijing 100083, PR China

The properties of synthesized side-chain liquid crystalline polymer (SCLCP)/liquid crystal (LC)/chiral dopant composites having a chiral nematic (N*) phase at room temperature were investigated by polarized optical microscopy (POM) and a UV/VIS/NIR spectrophotometer. The composite exhibited a planar texture after it was filled into cells under homogeneous boundary conditions and it was transparent. When an electric field was applied to the composite, a focal conic texture was formed and the composite became light scattering. After the electric field was turned off, the light-scattering state remained stable for some time, i.e. the light-scattering state exhibited a memory effect. The focal conic texture changed into the planar texture when the composite was heated and the composite became transparent again. Therefore, the composite had electrically induced and thermally erased properties. The SCLCP had some influence on the memory effect and on the thermo-electro-optical properties of the composite.

1. Introduction

A chiral nematic liquid crystal (N*-LC) can exhibit either a planar texture or a focal conic texture [1]. In the planar texture, all the helical axes are perpendicular to the cell surfaces, whereas they are randomly arranged in the focal conic one. An N*-LC with a planar texture will be transparent if the pitch length is much larger or smaller than the wavelength of visible light [2]. In contrast, an N*-LC with a focal conic texture shows strong light scattering due to the mismatch of refractive index between different domains. At zero fields, because there are many defects in the focal conic texture, the free energy of the focal conic texture is higher than that of the planar texture. Therefore, the planar texture is usually more stable than the focal conic texture. However, there is an energy barrier between them. When the pitch of N*-LC is short enough, the energy barrier is large enough between the textures and both the textures are stable at a zero field. Meanwhile, the free energy of the defects of the focal conic texture is pitch dependent [3]. The free energy increases with increasing pitch [4]. When the pitch is large enough, the free energy becomes too high, and the focal conic texture becomes more unstable. It becomes easier for the focal conic texture to change to the planar one. In other words, the memory effect (i.e. the stability of the focal conic texture) is pitch dependent. So far only these effects are understood, but much about the energy of the defects in N*-LC has not been thoroughly studied [5].

Recently, resulting from the stabilities of the planar and the focal conic textures at zero field, some kinds of N*-LC devices with two stable states have been investigated [6–10]. This kind of device has attracted much attention because power consumption can be reduced by two stable states, especially when the device does not require a frequent update [11]. These devices are promising for use in e-books or other low-power devices. Once displayed, the information can be memorized for a long time, ranging from seconds up to years, depending on the requirement of the application. One of the widely studied bistable N*-LC devices is the dual-frequency driven mechanism [12–14]. The N*-LC can be changed between the planar and the focal conic textures by applying electric fields with different frequencies. However, the driving voltage applied to make the focal conic texture change to the planar one is usually larger than $100\,V_{rms}$ [12], which is rather high. To satisfy the various practical applications, Yang *et al.* have developed several LC materials with thermally addressable and electrically erasable characteristics [15,

*Corresponding author. Email: yanghuai@mater.ustb.edu.cn

16]. Recently, a novel LC device with electrically addressable and thermally erasable characteristics using an LC/chiral dopant composite was also prepared [17].

To our knowledge, little work has been carried out on the effect of a side-chain liquid crystalline polymer (SCLCP) on the properties of electrically addressable and thermally erasable N*-LC devices. Therefore, in this study, SCLCP/LC/chiral dopant composites, which have a chiral nematic (N*) phase at room temperature, were prepared and the effects of the SCLCP on the memory effect and the thermo-electro-optical properties of the composite studied.

2. Experimental

2.1. Materials

A smectic A (SmA) SCLCP [PS(4BC/DM)], a nematic LC (SLC-1717) and a chiral dopant (CB-15) were used as components of the SCLCP/LC/chiral dopant composites. SLC-1717 and CB-15 were purchased from Slichem Liquid Crystal Material Co., Ltd. and Merck Co., Ltd., respectively and used without any purification. Figure 1 shows the chemical structure and some physical parameters of these materials. PS(4BC/DM) was synthesized according to a reported method [18]. The purity and the molecular weight of PS(4BC/DM) were measured by GPC, and the block ratio was
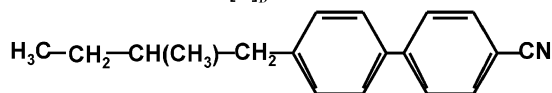
1. Liquid crystalline copolymer:
Mn=8000,Mw=10,270
PS[4BC/DM](n=12) m=4,n=x+y=12,x/y=52.5/47.5
$\overline{M}n=8000, \overline{M}w=10,270, \overline{M}w/\overline{M}n=1.28$
$S_A - 337 - I (Tg = 254K)$
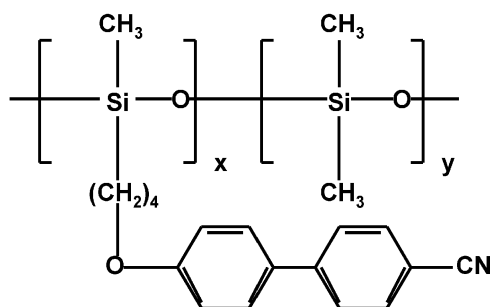
2. Chiral dopant : CB-15 (Merck Co., Ltd.)
right-handed helix $[\alpha]_D^{20} = +13$

3. LC: SLC-1717 (Slichem Liquid Crystal Material Co., Ltd.)
K-233.0-N-365.0-I

Figure 1.　Chemical structure and physical properties of the materials used.

determined by NMR and FTIR. The PS(4BC/DM)/SLC-1717/CB-15 composites were synthesized by a solvent cast method from acetone solutions.

2.2. Treatment of homogeneous orientation

To obtain homogeneous alignment, a 3.0 wt % polyvinyl alcohol (PVA) aqueous solution was coated onto the ITO-coated surfaces by spinning casting. The deposited film was dried at 353.2 K for about 30 min, and subsequently rubbed with a textile cloth under a pressure of $2.0 \, g \, cm^{-2}$ along one direction.

2.3. Fabrication of cells

Polyethylene terephthalate (PET) films of 24 μm thickness were used as cell spacers, and the composites were filled into the cells by capillary action in their isotropic (I) phases.

2.4. Measurements of pitch lengths

The pitch lengths of the N* phases of the composites were measured by the Cano wedge technique [19]. In this measurement, a wedge-shaped cell with a wedge angle, α, was used and the inner surfaces of its two glass substrates were treated to provide a homogeneous alignment of LC molecules. After the composite was filled into the cell in the isotropic phase and then cooled to the N* phase, at some temperature a Grandjean–Cano texture formed with disclination lines separated by a distance *l*. The pitch length *P* is determined from $P = 2\alpha l$ at that temperature.

2.5. Observation of the textures of composites

The textures of the composite were observed by polarized optical microscopy (POM) using an Olympus BX51.

2.6. Measurements of electro-optical effects

The electro-optical properties of the composites were measured by a liquid crystal display parameters tester (LCT-5016C, Changchun Lianchen Instrument Co., Ltd). The transmittance of air was normalized as 100%.

2.7. Measurements of thermo-optical effects

The temperature dependence of the transmittance for the composites was obtained using a UV/VIS/NIR spectrophotometer (JASCO V-570). The wavelength of the incident light was 589 nm. The transmittance of air was normalized as 100%.

3. Results and discussion

Table 1 lists the compositions of the studied samples. The ratio of CB15 to SLC1717 was 1:24 for samples A_1–D_1 and 1:11.5 for samples A_2–D_2.

Figure 2 shows the temperature dependence of the pitch lengths of the N* phase of samples A_1–D_1 and A_2–D_2. It was found that the pitch length of the samples was inversely proportional to the content of CB15 [2] and little affected by the content of PS(4BC/DM). The pitch length increased with increasing temperature.

Figure 3 shows POM photos of the initial states of the samples at room temperature. For all the samples, they adopted a planar texture due to the fact that the inner surfaces of the cells had been treated for homogeneous orientation of LC molecules. PS(4BC/DM) did not significantly affect the initial planar texture.

Figure 4 shows the PS(4BC/DM) dependence of the transmittances of the initial states of samples A_1–D_1

Table 1. The compositions of samples A_1–D_2.

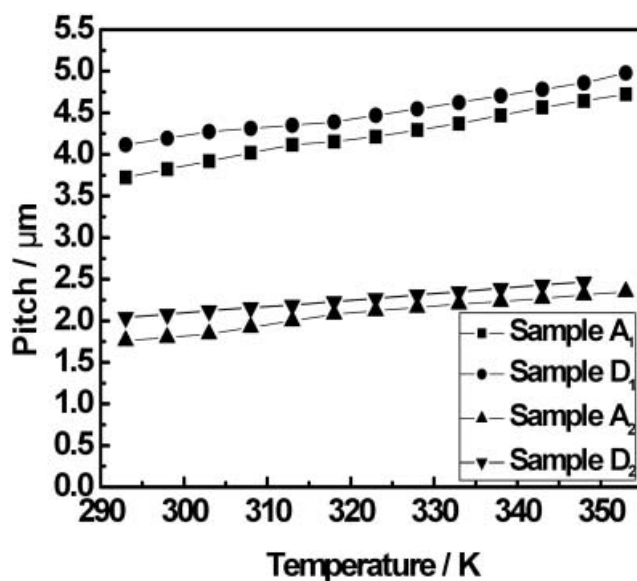| Sample	PS(4BC/DM)/CB15/SLC1717/wt %
A_1	0.0/4.0/96.0
B_1	4.0/3.8/92.2
C_1	8.0/3.7/88.3
D_1	12.0/3.5/84.5
A_2	0.0/8.0/92.0
B_2	4.0/7.7/88.3
C_2	8.0/7.4/84.6
D_2	12.0/7.0/81.0

Figure 2. Plots of temperature versus helical pitch for the samples A_1, D_1 and A_2, D_2.
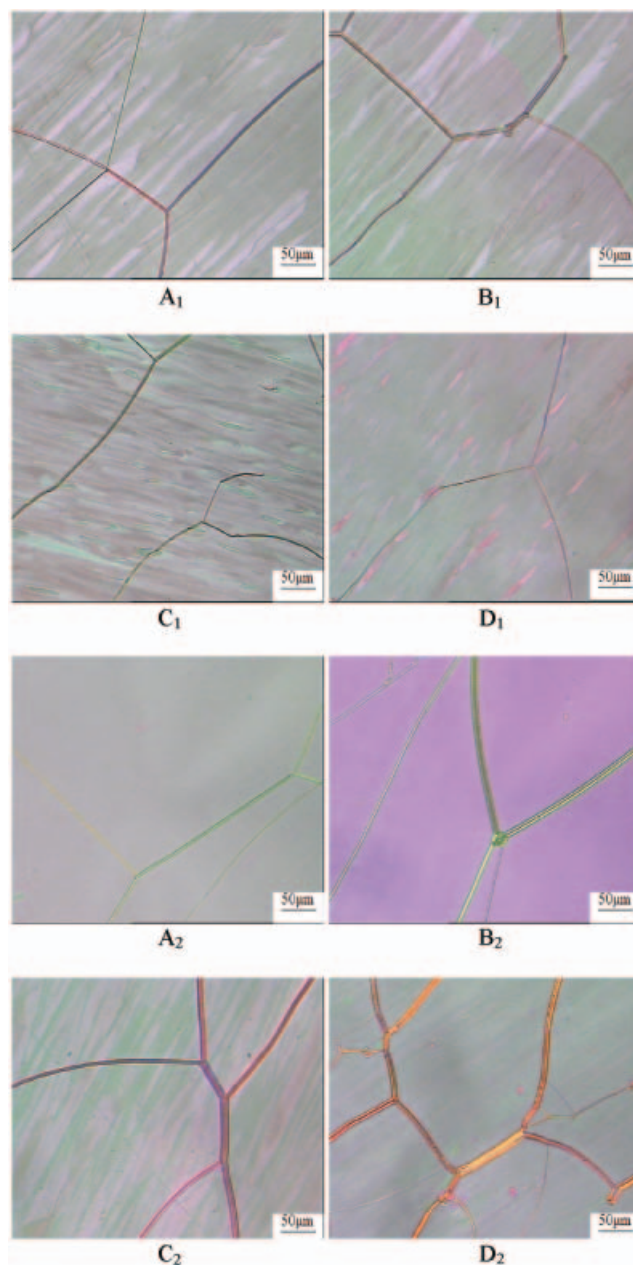

Figure 3. POM photos of the textures of the initial states of samples A_1–D_2 at room temperature.

and A_2–D_2. It can be seen that the transmittance of the initial states of the samples was not affected by PS(4BC/DM).

Figure 5 shows the dependence on applied voltage of the transmittances of samples A_1–D_1 and A_2–D_2. When the applied voltage was larger than the threshold voltage, the transmittances of the samples began to decrease, changing from the transparent state to the light-scattering state. POM observation showed that the planar textures began to change to focal conic ones.
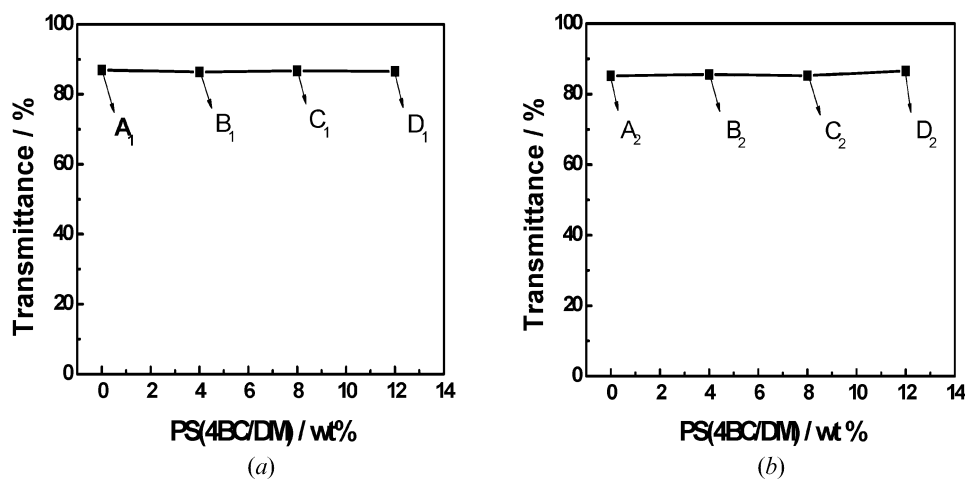
Figure 4.　Plots of content of PS(4BC/DM) versus initial transmittance for samples A_1–D_1 (a) and samples A_2–D_2 (b).

Samples A_1–D_1, with a lower content of CB15, had larger pitch lengths than samples A_2–D_2 with higher CB15 content [2]. Hence, the threshold voltages of samples A_1–D_1 were lower than those of samples A_2–D_2 [20].

The light-scattering state of the cells remained to a certain extent after the electric field was turned off. Figure 6 shows the time dependence of the transmittances of the light-scattering states of the samples. The transmittances of samples A_1–D_1 increased more dramatically with time than those of the samples A_2–D_2. Figure 6a shows that after 2 h the transmittance increased from 26.8% to 79.9%, from 15.8% to 56.8%, from 12.4% to 52.2% and from 10.6% to 43.9% for samples A_1, B_1, C_1 and D_1, respectively. The difference in transmittance after 2 h was 53.1%, 40.0%, 39.8% and 33.3%, respectively. Figure 6b shows that after 2 h the

transmittance increased from 5.6% to 12.2%, from 4.2% to 9.4%, from 3.7% to 8.4% and from 6.8% to 9.8% for samples A_2, B_2, C_2 and D_2, respectively. The difference in transmittance after 2 h was 6.6%, 5.2%, 4.7%, 3.0%, respectively. The memory effect of samples A_1, B_1, C_1 and D_1 increased in that sequence, and the same tendency was observed for samples A_2, B_2, C_2 and D_2.

The easier change from focal conic texture to planar texture for the former samples compared with the latter samples, as demonstrated by POM observation, confirmed that the memory effects of samples A_2, B_2, C_2 and D_2 were larger than those of samples A_1, B_1, C_1 and D_1. The former samples had weaker memory effect than the latter samples due to their longer pitch length. The results confirmed that the memory effect of the focal conic texture is dependent on pitch length. The memory effects of samples A_1 and A_2 were somewhat weaker
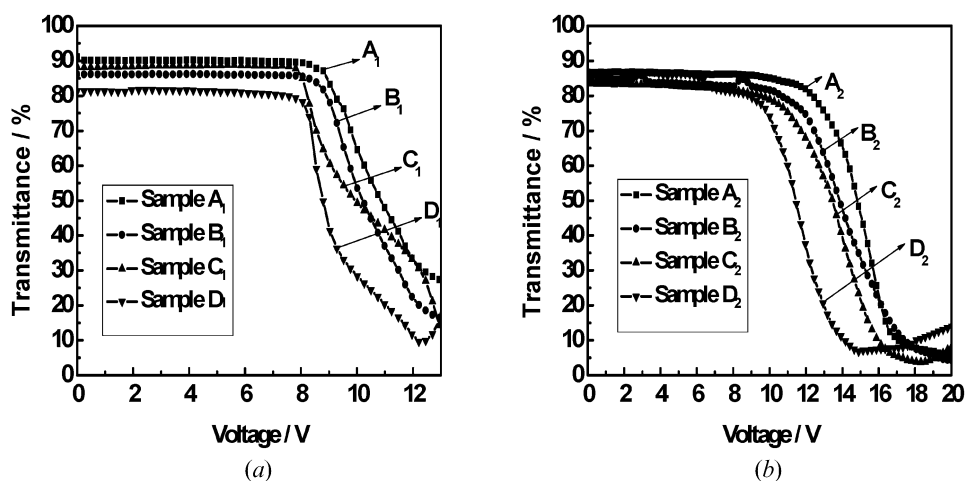

Figure 5.　Plots of applied voltage (100 Hz) versus transmittance for samples A_1–D_1 (a) and samples A_2–D_2 (b) at room temperature.
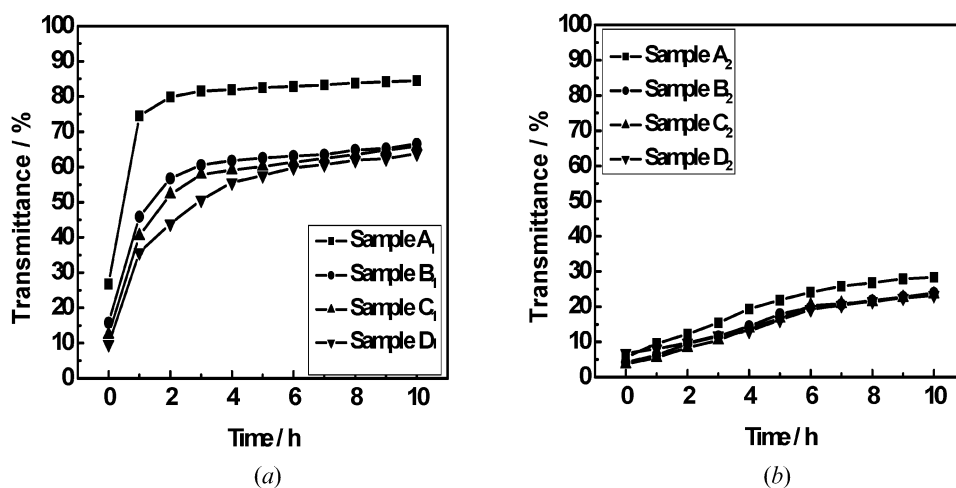
Figure 6.   Plots of time versus transmittance for samples A_1–D_1 (a) and samples A_2–D_2 (b) at room temperature.
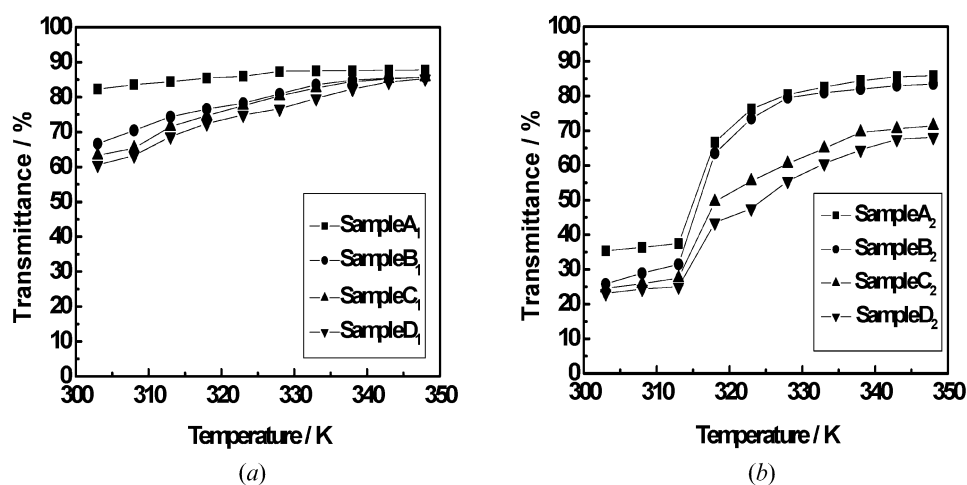

Figure 7.   Plots of temperature versus transmittance for samples A_1–D_1 (a) and samples A_2–D_2 (b).

than samples B_1–D_1 and B_2–D_2, respectively, and the memory effects of samples A_1, B_1, C_1 and D_1 became stronger in that sequence. Hence, the addition of PS(4BC/DM) resulted in the memory effect becoming a little stronger. Because the backbone of PS(4BC/DM) tends to be randomly distributed, the tendency for the composites to form focal conic texture increased with increasing content of PS(4BC/DM) [21].

Measurements of the thermo-optical properties of the composites were obtained using a UV/VIS/NIR spectro-photometer after the electric field was turned off for 12 h. Figure 7 shows the temperature dependence of the transmittances of the samples A_1–D_1, and A_2–D_2 at a heating rate is kept of $1 \, K \, min^{-1}$. The transmittances of the samples increased with increasing temperature, i.e. all the samples had the an increased tendency to change

from the focal conic to the planar texture with increasing temperature [17]. This is because the pitch lengths also increased with increasing temperature. The light-scattering intensities of the initial states increased and the tendency of the samples to change from the focal conic to the planar texture decreased with increasing content of PS(4BC/DM), due to the fact that the backbone of PS(4BC/DM) is randomly distributed, as mentioned above.

4.   Conclusion

The electrically induced and thermally erased properties of synthesized side chain liquid crystalline polymer (SCLCP)/liquid crystal (LC)/chiral dopant composites have been investigated by polarized optical microscopy

(POM) and a UV/VIS/NIR spectrophotometer. The results show that the focal conic textures of PS(4BC/DM)/CB15/SLC1717 composites became more stable with decreasing pitch length and the memory effect of the composites increased with decreasing pitch length. The backbone of PS(4BC/DM) tended to adopt a random distribution, as confirmed by the observation that the memory effect increased with increasing PS(4BC/DM) content. The memory effect and the thermo-electro-optical properties of the composites can be optimized by optimizing the contents of CB15 and PS(4BC/DM).

Acknowledgements

References

[1] I. Dierking. *Textures of Liquid Crystals*, pp. 56, Wiley-VCH, Weinheim (2003).
[2] P.G. de Gennes, J. Prost. *The Physics of Liquid Crystals*, p. 263, Clarendon, Oxford (1993).
[3] F. Zhang, D.K. Yang. *Phys. Rev. E*, **66**, 041701 (2002).
[4] S. Chandrasekhar. *Liquid Crystals,* second edn, pp. 248–258, Cambridge University Press, New York (1997).
[5] G.P. Crawford, S. Zumer. *Liquid Crystals in Complex Geometries*, pp. 124–126, Taylor & Francis, London (1996).
[6] W.C. Yip, H.S. Kwok. *Jap. J. appl. Phys. Pt. 1*, **40**, 4916 (2001).
[7] R.Q. Ma, D.K. Yang. *J. Soc. Inf. Display*, **7**, 61 (1999).
[8] T.Z. Qian, Z.L. Xie, H.S. Kwok, P. Sheng. *Appl. Phys. Lett*, **71**, 596 (1997).
[9] I. Dozov, M. Nobili, G. Durand. *Appl. Phys. Lett*, **70**, 1179 (1997).
[10] X.J. Yu, H.S. Kwok. *Appl. Phys. Lett*, **85**, 3711 (2004).
[11] I. Dozov. *SID Int. Symp. Dig. Tech. Pap*, **34**, 946 (2003).
[12] M. Xu, D.K. Yang. *Appl. Phys. Lett*, **70**, 720 (1997).
[13] J.S. Hsu, B.J. Liang, S.H. Chen. *Appl. Phys. Lett*, **85**, 5511 (2004).
[14] Y.Q. Lu, X. Liang, Y.H. Wu, F. Du, S.T. Wu. *Appl. Phys. Lett*, **85**, 3354 (2004).
[15] H. Yang, H. Kikuchi, T. Kajiyama. *Liq. Cryst*, **27**, 1695 (2000).
[16] H. Yang, H. Kikuchi, T. Kajiyama. *Liq. Cryst*, **29**, 1141 (2002).
[17] J. Geng, C. Dong, H. Yang. *Appl. Phys. Lett*, **89**, 081130 (2006).
[18] H. Finkelmann, U. Kiechle, G. Rehage. *Mol. Cryst. liq. Cryst*, **94**, 343 (1983).
[19] R. Cano. *Bull. Soc. Fr. Mineral*, **91**, 20 (1968).
[20] G. Di Profio, J. Lanzo, F.P. Nicoletta, et al. *Appl. Phys. Lett*, **79**, 4512 (2001).
[21] H. Yang, H. Kikuchi, T. Kajiyama. *J. appl. Polym. Sci*, **73**, 623 (1999).